

# Behavior of high-strength concrete columns subjected to blast loading

T.D. Ngo, P.A. Mendis, D. Teo & G. Kusuma  
*University of Melbourne, Australia*

**ABSTRACT:** This paper presents the current analytical investigation at the University of Melbourne on the behavior of high-strength concrete (HSC) columns subjected to severe blast loadings. The variables considered were the magnitude of the blast, the concrete strength (40MPa for normal strength concrete and 80MPa for HSC). A constitutive law to model the strain-rate-dependent engineering properties of HSC is proposed. Dynamic stress-strain relations which differ considerably from the corresponding static relations are derived for the investigated load histories and are modeled with the proposed dynamic constitutive law. The effects of reinforcement detailing, geometry, and loading conditions on the dynamic behaviour of high-strength concrete columns were investigated by the Finite Element Explicit code LS-DYNA3D. A case study was carried out to assess the performance of a ground floor RC column of a typical office building under a bomb blast. It was found that HSC columns perform better than NSC columns (with the same axial load capacity) when subjected to extreme impulsive loading.

## 1 INTRODUCTION

High-strength concrete (HSC) is a relatively new construction material. Technology for producing high-strength concrete has sufficiently advanced that concretes with compressive strengths up to 100 MPa are commercially available and strengths much higher than that can be produced in laboratories. High-strength concrete offers significantly better structural engineering properties, such as higher compressive and tensile strengths, higher stiffness, better durability, when compared to the conventional normal strength concrete (NSC).

Responding to the threat of terrorist attacks around the world, structural engineers are seeking new methods of assessment and prevention of high-risk facilities. Some studies on impact resistance of HSC beams and plates (Jensen 1998, Banthia 1987) have found that HSC performs better than NSC when subjected to impulsive loading. Thus, HSC is an obvious choice in protecting buildings against the extreme loading conditions. However there is still a serious lack of knowledge of the performance of HSC structural members in extreme events like a bomb blast or a high velocity impact. This paper presents the details of an ongoing study on the behavior of HSC columns under blast loading. A simple assessment procedure is proposed to predict potential damage to these members subjected to this extreme loading.

## 2 BLAST LOADING

The threat for a conventional bomb is defined by two equally important elements, the bomb size (or charge weight ( $W$ ), which is normally measured using the equivalent amount of TNT), and the standoff distance ( $R$ ) between the blast source and the target. For example, the blast occurred at the basement of World Trade Centre in 1993 had the charge weight of 816.5 kg TNT. The Oklahoma bomb in 1995 had a charge weight of 1814 kg at a stand-off distance of 4.75m (Longinow, 1996).

With the detonation of a mass of TNT at or near the ground surface, the peak blast pressures resulting from this hemispherical explosion decay as a function of the distance from the source as the expanding shock front dissipates with range. The incident peak pressures are amplified by a reflection factor as the shock wave encounters an object or structure in its path. The reflected pressure is at least twice that of the incident shock wave and is proportional to the strength of the incident shock, which is proportional to the charge weight.

The blast pressure decays exponentially and eventually becomes negative as shown in Fig.1. This then subjects the building to pressures acting in the direction opposite (suction pressure) to that of the original shock front.

Peak blast loads may be several orders of magnitude larger than the largest loads for which conven-

tional buildings are designed. For example, for the Oklahoma bomb in 1995, the peak pressure of the shock front at a distance of 10 m from the point of detonation is approximately 13.6 MPa (compared to a pressure of 1.24 kPa produced by 45m/s wind). The peak pressure, however, drops off rapidly with distance.

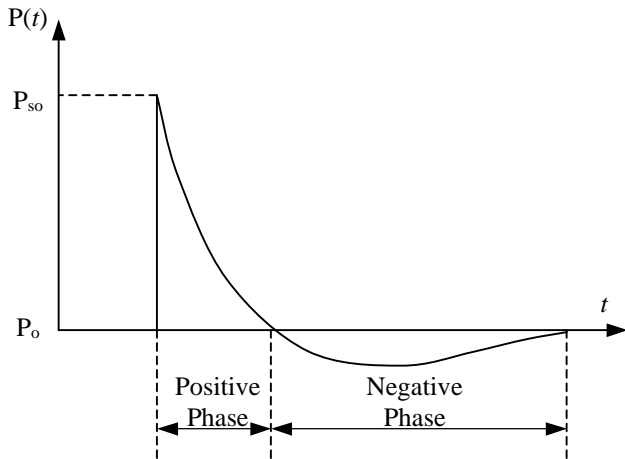


Figure 1. Blast wave pressure – Time history

The difference between technical hazards (accidental or terrorist) and other natural hazards is that the risks of technical hazards are very hard to quantify. For these types of hazards the performance-based approach can be used as a rational method for assessment or design of buildings against extreme events. The performance level – hazard matrix is shown in Figure 2.

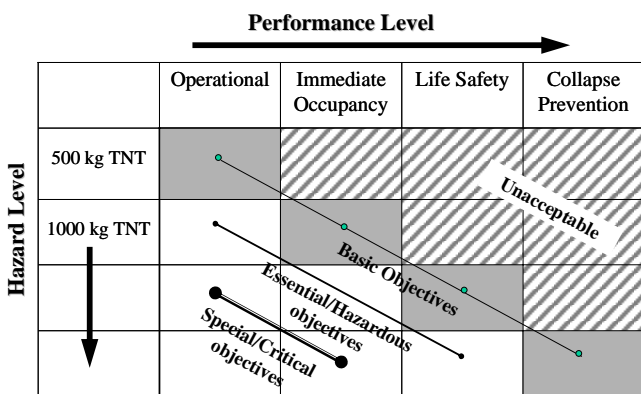


Figure 2. Performance-based approach

Table 1. Peak reflected overpressures (MPa) with different W-R combinations (TM5-1300, 1990)

R	W	100kg	500kg	1 ton	2 ton
		TNT	TNT	TNT	TNT
1m		165.8	354.5	464.5	602.9
2.5m		34.2	89.4	130.8	188.4
5m		6.65	24.8	39.5	60.19
10m		0.85	4.25	8.15	14.7
15m		0.27	1.25	2.53	5.01
20m		0.14	0.54	1.06	2.13
25m		0.09	0.29	0.55	1.08
30m		0.06	0.19	0.33	0.63

### 3 MATERIAL BEHAVIOURS AT HIGH STRAIN-RATE

In the event of extreme blast load, building structures are expected to undergo large inelastic deformation. Hence the ultimate capacity of the building depends greatly on the ability of structural members to deform inelastically under extreme overload, thereby dissipating large amounts of energy, prior to failure. Key parameters that describe the full-range ductile behaviour of reinforced concrete flexural members are: 1) rotation capacity of the plastic hinge,  $\theta_u$ ; 2) hinge length,  $l_p$ ; and 3) softening slope parameter,  $a$ . In the interest of proper structural designs and safety, knowledge of these three key ductility parameters is essential. The collapse load of a frame structure was shown by Mendis (1986) to be significantly influenced by these parameters. An increase in hinge length increases the collapse load. An increase in rotation capacity has the same effect, but an increase in softening slope (i.e. steeper slope) reduces the collapse load (Mendis, 1986).

Full-range behaviour of concrete flexural members can be idealized as a trilinear fit of the moment curvature ( $M-\phi$ ) diagram, as shown in Fig.3, consisting of elastic, plastic, and softening portions. The member flexural ductility has been defined as:

$$\Psi_u = \frac{\phi_u}{\phi_y} \quad (1)$$

where  $\phi_u$  is the curvature corresponding to a moment equal to 80 percent of  $M_u$ .

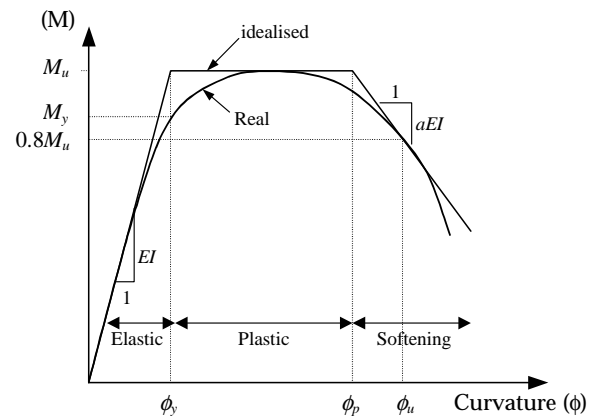


Figure 3. Real and idealized full-range moment-curvature ( $M-\phi$ ) relationship

Full-range analysis including post-peak behaviour has been recommended in many seismic design guidelines such as FEMA 273/274, FEMA 356/357, FEMA 368/369, and FEMA 306/307/308. Considerations of softening phenomenon and full-range analysis become extremely important in design where large deformations are expected such as blast resistant design.

#### Strain-rate effect

For reinforced concrete structures subjected to blast or impact effects, response at very high strain rates (up to  $1000 \text{ s}^{-1}$ ) is often sought. At these high

strain rates, the strength of concrete and steel reinforcing bars can increase significantly. While the dynamic stiffness does not change very much compared to the static stiffness, the stresses that are sustained for a certain period under dynamic conditions may gain values that are remarkably higher than the static compressive strength (Fig. 4). Strength magnification factors as high as 4 in compression and up to 6 in tension for strain rates in the range of  $10^2$ – $10^3$  /sec have been reported (Grote et al., 2001). Fu et al. (1992) found that in many tests involving concrete members, the flexural mode of failure was observed at relatively slow loading rates, while at high loading rates the shear failure or mixed mode failure became the main dominant failure mode.

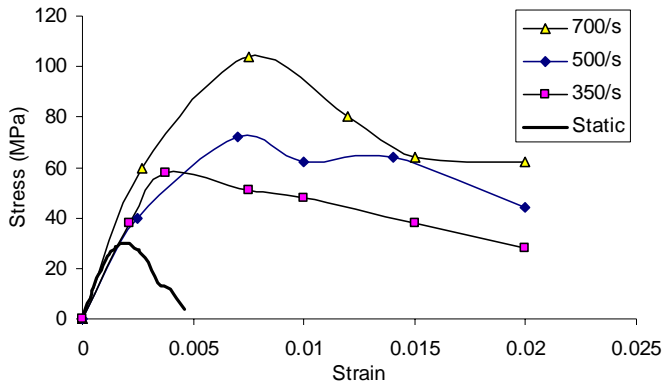


Figure 4. Stress-strain curves of concrete at different strain-rates (Gary et al., 1990)

### Material model for concrete

Stress-strain relationship of concrete under increasing rates of strain has been observed to be quite different from that of concrete under static load due to the changes in (1) Compressive strength; (2) strain at ultimate stress; and (3) the softening slope of the descending branch. Several concrete models have been proposed based on results of impact tests.

Scott et al. (1982) developed a stress-strain model for confined concrete under compression and included the effect of strain rates by a multiplying factor which influences the concrete strength, strain at peak strength, and slope of the descending portion of the stress-strain curve. However, the Scott model was based on a relatively low strain rate data ranging from a quasi-static rate of  $3.3 \times 10^{-6} \text{ s}^{-1}$  to  $0.0167 \text{ s}^{-1}$ .

Soroushian et al. (1986) revised the Scott's empirical model by introducing three new parameters  $K_1$ ,  $K_2$ ,  $K_3$  which take into account the effects of concrete confinement due to the presence of transverse reinforcement, the effects of different strain rates on compressive strength of concrete and the effects of different strain rates on the strain at maximum stress respectively.

Based on calibration of experimental results for high strength concrete, Mendis et al. (2000) modified the Scott's stress-strain model for concrete under static load by extending the validity of the model to both normal strength concrete (NSC) and high

strength concrete (HSC). This model can be applied to concrete strength up to 100 MPa.

The Modified Scott Model is described by Eqs. 2 to 6 and Fig. 5. More details of the model can be found elsewhere (Mendis et al., 2000). For unconfined concrete the equation which defines the parabolic ascending portion of the stress-strain curve is expressed as:

$$f = f'_c \left[ \frac{2\varepsilon}{\varepsilon_c} - \left( \frac{\varepsilon}{\varepsilon_c} \right)^2 \right] \quad \text{for } \varepsilon \leq \varepsilon_c \quad (2)$$

$f'_c$  - characteristic concrete compressive strength (MPa).

The equation for the linear descending portion is given below:

$$f = f'_c - Z'_m (\varepsilon - \varepsilon_c) \geq f_{res} \quad \text{for } \varepsilon > \varepsilon_c \quad (3)$$

but not less than  $f'_c f_{res}$

where,

$$Z'_m = f'_c \frac{0.009 f'_c + 0.275}{3 + 0.29 f'_c - \varepsilon_c} \geq 0 \quad (4)$$

$$\varepsilon_c = \frac{4.26}{\sqrt[4]{f'_c}} \frac{f'_c}{E_c}, \quad \text{where } E_c \text{ is the Modulus of Elasticity of concrete (MPa)} \quad (5)$$

Elasticity of concrete (MPa)

$$f_{res} = f'_c (0.28 - 0.0032 f'_c) \geq 0 \quad (6)$$

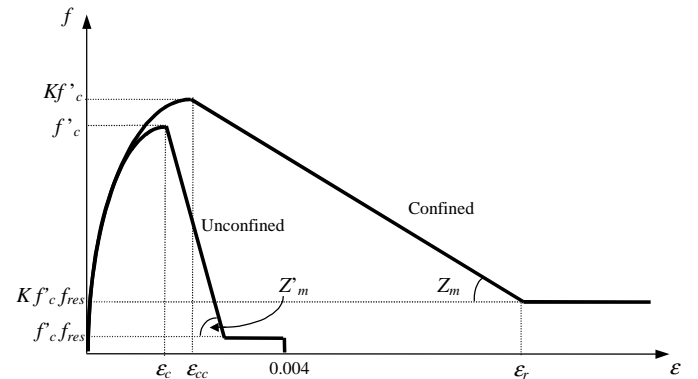


Figure 5. The Modified Scott Model for concrete under static load (Mendis et al., 2000)

### Strain-rate dependent concrete model

Based on a few test results available from literature (Gary et al. 1990, Grote et al. 2001) which involved high velocity impact tests using Hopkinson Bar apparatus and through a rigorous calibration process the Modified Scott Model has been revised to cover strain rate up to  $700 \text{ s}^{-1}$ . A new strain-rate dependent model is proposed by the authors for concrete under dynamic load which can take into account the strain-rate effect by incorporating multiplying factors for increases in the peak stress, strain at peak strength, and the variation in the softening slope.

For the increase in peak stress ( $f'_c$ ), a dynamic increase factor,  $K_d$ , is introduced using the CEB-FIP (1990) model for strain-rate enhancement of concrete (Fig. 6) as follows:

$$K_d(\dot{\epsilon}) = \left( \frac{\dot{\epsilon}}{\dot{\epsilon}_s} \right)^{1.026\alpha} \quad \text{for } \dot{\epsilon} \leq 30s^{-1} \quad (7)$$

$$K_d(\dot{\epsilon}) = \gamma \left( \frac{\dot{\epsilon}}{\dot{\epsilon}_s} \right)^{1/3} \quad \text{for } \dot{\epsilon} > 30s^{-1} \quad (8)$$

where:

$\dot{\epsilon}$  = strain rate

$\dot{\epsilon}_s = 30 \times 10^{-6} s^{-1}$  (quasi-static strain rate)

$\log \gamma = 6.156\alpha - 2$

$\alpha = 1/(5 + 9f'_c / f_{co})$

$f_{co} = 10 \text{ MPa} = 1450 \text{ psi}$

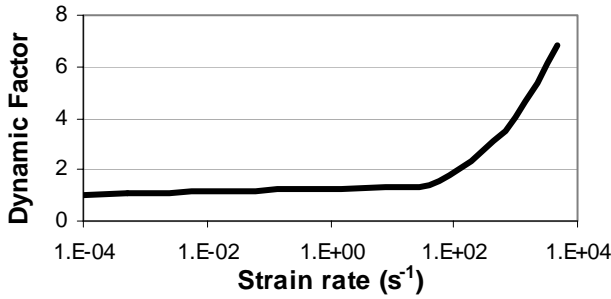


Figure 6. Dynamic Magnification Factor for peak stress of concrete (CEB-FIP model)

The strain at peak stress also increases from  $\epsilon_c$  to  $\epsilon_{dc}$ , which is also strain-rate dependent:

$$\epsilon_{dc} = (0.12 K_d^3(\dot{\epsilon}) + 0.76) \epsilon_c = K^* \epsilon_c \quad (9)$$

The softening slope,  $Z_d$ , which has been calibrated with experimental results, is proposed as:

$$Z_d = \frac{K_d f'_c Z}{\frac{3 + 0.29 f'_c}{145 f'_c - 1000} + \frac{3}{4} \rho_s \sqrt{\frac{h''}{s_h}}} \left( \frac{\dot{\epsilon}}{\dot{\epsilon}_s} \right)^{-0.1} \geq 0 \quad (10)$$

where:

$\rho_s$  = volumetric ratio of hoop reinforcement to concrete core measured to outside of the hoops,

$h''$  = width of concrete core measured to outside of peripheral hoop (mm),

$s_h$  = centre-to-centre spacing of hoop sets (mm),

The proposed Modified Scott Model for dynamic load can be expressed in Eqs. 11 & 12 as:

$$f = K_d f'_c \left[ \frac{2\epsilon}{\epsilon_{dc}} - \left( \frac{\epsilon}{\epsilon_{dc}} \right)^2 \right] \quad \text{for } \epsilon \leq \epsilon_{dc} \quad (11)$$

$$f = K_d f'_c - Z_d (\epsilon - \epsilon_{dc}) \quad \text{for } \epsilon > \epsilon_{dc} \quad (12)$$

#### Material model for reinforcing steel

Under high strain rates, both the yield and ultimate stresses of reinforcing bars increase. A comprehensive review of loading rate effects on reinforcing steel by Malvar (1998) indicated that the modulus of elasticity and ultimate strain remain nearly constant, but that other bar properties, such as

yield stress and yield strain, increase with strain rate. The ultimate stress increase is less significant (up to 5% at high strain rates). The dynamic increase factor (DIF) for yield strength ( $f_y$ ) and ultimate strength ( $f_{su}$ ) recommended by Malvar (1998) is adopted in this study.

#### 4 CASE STUDY

A ground floor column (6.4m high) of a multi-storey building (modified from a typical building designed in Australia) was analysed in this case study (see Fig. 7).

The parameters considered were the concrete strength (40MPa for NSC column and 80 MPa for HSC column) and spacing of ligatures (400mm for ordinary detailing-OMRF and 100mm for special seismic detailing-SMRF). It has been found that with increasing concrete compressive strength, the column size can be effectively reduced. In this case the column size was reduced from 500 x 900 mm for the NSC column down to 350 x 750 for the HSC column (Table 2) while the axial load capacities of the two columns are still the same.

The blast load was calculated based on data from the Oklahoma bombing report (ASCE 1996) with a stand off distance of 11.2m. The simplified triangle shape of the blast load profile was used (see Fig. 8). The duration of the positive phase of the blast is 1.3 milliseconds.

The 3D model of the column (see Fig. 9) was analysed using the nonlinear explicit code LS-Dyna 3D (2002) which takes into account both material nonlinearity and geometric nonlinearity. The strain-rate-dependent constitutive model proposed in the previous section was adopted. The effects of blast was modelled in the dynamic analysis to obtain the deflection-time history of the column.

Table 2. Concrete grades and member sizes

Column	Sizes	$f'_c$ (MPa)	Ligature Spacing
NSC	500x900	40	400mm and 100mm
HSC	350x750	80	400mm and 100mm

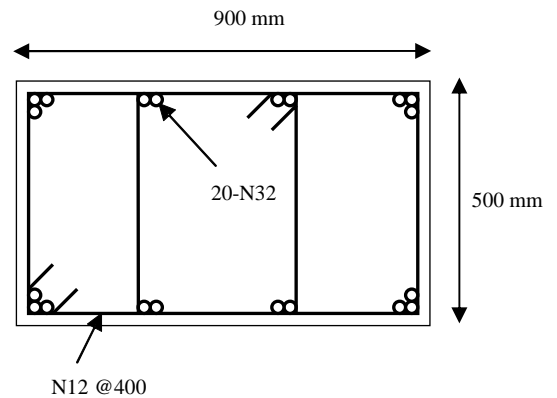


Figure 7. Cross section of the NSC column – Ordinary detailing (400 mm ligature spacing).

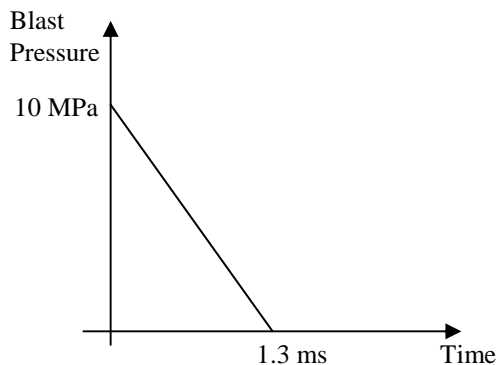


Figure 8. Blast loading

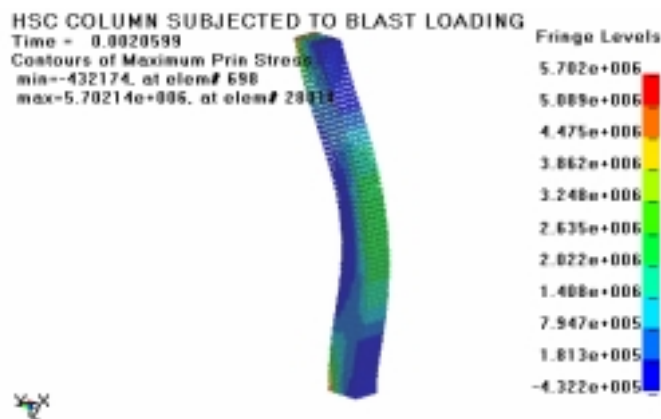


Figure 9. 3D model of the column using Explicit code LS-Dyna

The lateral deflection at mid point versus time history of two columns made of NSC and HSC are shown in Figs. 10 and 11. The graphs clearly show the lateral resistance of the columns. It can be seen that under this close-range bomb blast both columns failed in shear. However, the 80MPa columns with reduced cross section have a higher lateral deflection, which shows a better energy absorption capacity compared to that of the 40 MPa columns (see Fig. 12 and Table 3).

It can be seen from Figs. 10 and 11 that the effect of shear reinforcement is also significant. The ultimate lateral displacements at failure increase from 45mm (400 mm ligature spacing) to 63mm (100mm ligature spacing) for the HSC column. Those values for the NSC column are 20mm and 32mm, respectively.

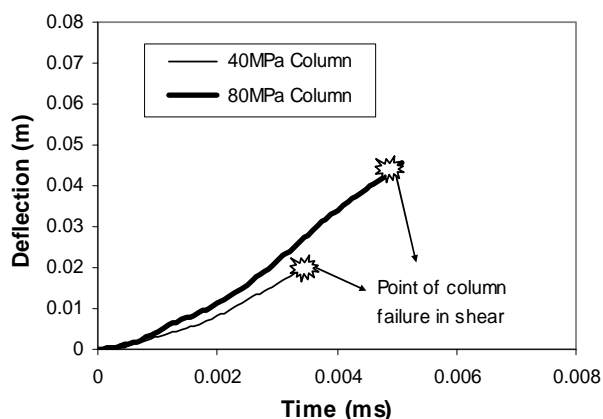


Figure 10. Lateral Deflection -Time history at mid point of column with 400mm ligature spacing (OMRF).

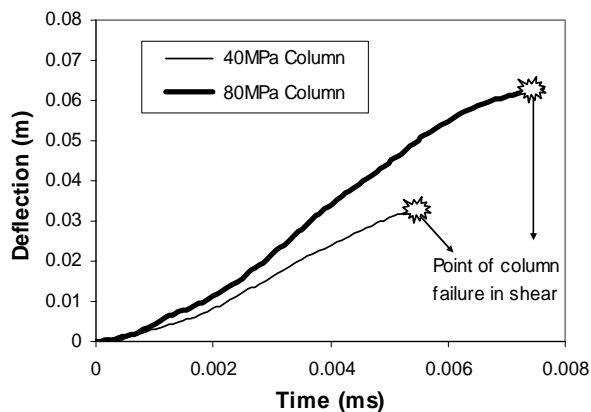


Figure 11. Lateral Deflection -Time history at mid point of column with 100mm ligature spacing (SMRF).

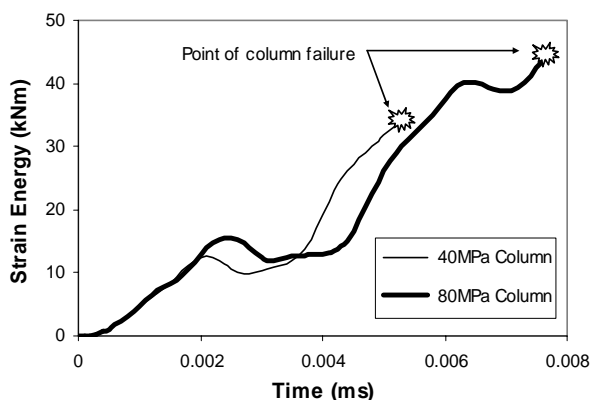


Figure 12. Comparison of energy absorption capacities (100mm ligature spacing).

Table 3. Energy absorptions at failure of HSC and NSC columns

Column	400mm spacing	100mm spacing
NSC	12.0 kNm	33.9 kNm
HSC	27.6 kNm	43.5 kNm

## 5 EFFECT OF STRAIN-RATE ON DUCTILITY

It is evident that increasing the rate of loading will result in increases in strength and stiffness of concrete, yield strength of steel and load-carrying capacity of reinforced concrete flexural members. A parametric study has been carried out to investigate the effects of high strain-rate on the ductility of reinforced concrete members, and that effect on the flexural and shear capacities. The proposed strain-rate dependent model for concrete is adopted in this study. As shown in Fig. 13 the flexural capacity and the ductility of a reinforced concrete column were significantly increased due to the increase in yield strength of steel and compressive strength of concrete at high strain rate. The shear capacity of the column was calculated using the Modified Compression Field theory (Vecchio and Collins, 1986).

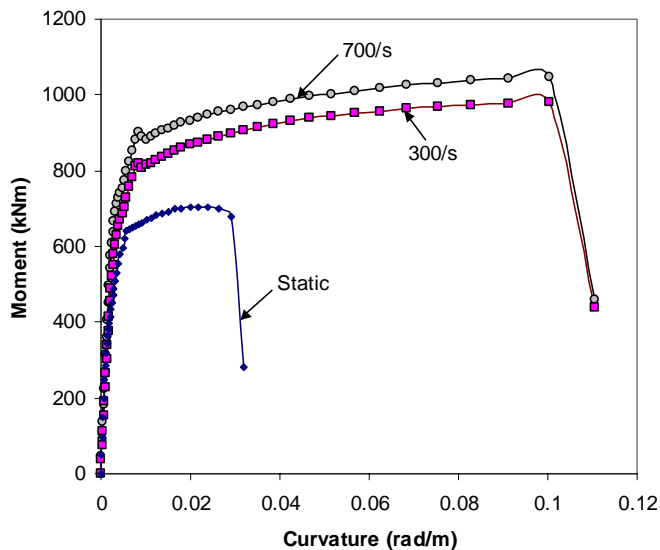


Figure 13.  $M-\phi$  curves of a cross-section of a column at different strain rates

Fig. 14 shows the increased ratio of flexural capacity ( $M_{u,dyn}/M_{u,stat}$ ) and shear capacity ( $V_{u,dyn}/V_{u,stat}$ ) at high strain rate compared to those capacities under static loading. It can be observed from Fig. 14 that the increase in flexural strength was greater than that of shear strength. Thus, the increase in the material strengths under dynamic conditions may lead to a shift from a ductile flexural failure to a brittle shear failure mode. This work is continuing at the University of Melbourne.

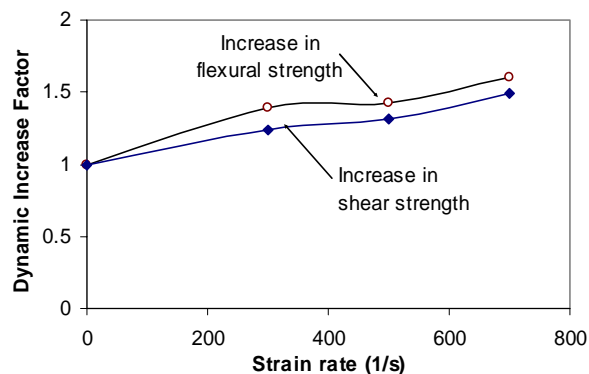


Figure 14. DIFs for flexural strength and shear strength of a column at different strain rates

## 6 CONCLUDING REMARKS

The study on the response of HSC and NSC columns subjected to a bomb blast is presented in this paper. A strain-rate-dependent constitutive model for concrete is proposed which is applicable to both normal strength and high strength concretes. Results from the study show that the impulsive loading is very different from the static loading in terms of the dynamic inertia effect and structural response. It is recommended that guidelines on abnormal load cases should be included in the current Australian Building Regulations and Design Standards.

It was found that shear failure was the dominant mode of failures for close-range explosion. HSC columns were shown to perform better than NSC columns (with the same axial load capacity) when

subjected to extreme impulsive loading; they also had higher energy absorption capacity. This study is continuing at the University of Melbourne.

## ACKNOWLEDGMENTS

The authors would like to thank the Victorian Partnership for Advanced Computing for financial support (Expertise Grant No. EPPNME073.2002) with this project.

## REFERENCES

- ASCE. 1995. The Oklahoma City Bombing, *Improving Building Performance through Multi-Hazard Mitigation*.
- Comité Euro-International du Béton, 1990. *CEB-FIP Model Code 1990*, Redwood Books, Trowbridge, Wiltshire, UK.
- Longinow, A., & Mniszewski, K.R. 1996. Protecting buildings against vehicle bomb attacks, *Practice Periodical on Structural Design and Construction*, V1, 1, pp 51-54.
- Prendergast, J. 1995. Oklahoma City Aftermath, *Civil Engineering - ASCE*, Vol. 65, No. 10, October 1995, pp. 42-45.
- FEMA 273/274. 1997. NEHRP guidelines for seismic rehabilitation of buildings. 1997 Edition. FEMA 356/357. 2000: USA.
- FEMA 368/369. 2000. NEHRP recommended provisions for seismic regulations for new buildings and other structures. USA.
- FEMA 306/307/308. 1998. NEHRP Evaluation and repair of earthquake damaged concrete and masonry buildings. USA.
- Fu, H.C., Erki, M.A. & Seckin, M. 1992. Review of Effects of Loading Rate on Reinforced Concrete. *Journal of the Structural Engineering, ASCE*, V 117, 12, pp. 3660-3679.
- Gary, G. 1990. Essais a grande vitesse sur béton. Problèmes spécifiques, *Rapport spécifique du GRECO*. GRECO Publisher, Paris (in French).
- Grote, D., Park, S., & Zhou, M. 2001. Dynamic behaviour of concrete at high strain rates and pressures. *Journal of Impact Engineering*, V25, pp. 869-886.
- LS-DYNA Version 960. 2002. Livermore Software Technology Corporation.
- Malvar LJ. 1998. Review of Static and Dynamic Properties of Steel Reinforcing Bars, *ACI Materials Journal*, V95, 5, pp. 609-616.
- Mendis, P.A. 1986. Softening of Reinforced Concrete Structures. Ph.D Thesis. Department of Civil Engineering, Monash University: Australia.
- Mendis, P.A., Pendyala, R., & Setunge, S. 2000. Stress-strain model to predict the full-range moment curvature behaviour of high-strength concrete sections. *Magazine of Concrete Research*, V52, 4, pp. 227-234.
- Scott, B.D., Park, R., & Priestley, M.J.N. 1982. Stress-Strain Behaviour of Concrete by Overlapping Hoops at Low and High Strain Rates. *ACI Structural Journal*, V19, 1, pp. 13-27.
- Soroushian, P., Choi, K., & Alhamad, A. 1986. Dynamic constitutive behavior of concrete, *ACI Structural Journal*, V 83, 2, pp. 251-258.
- TM5-1300. 1991. Structures to Resist the Effects of Accidental Explosions. US Army. USA.
- Vecchio, F.J., & Collins, M.P. 1986. The Modified Compression Field Theory for Reinforced Concrete Elements Subjected to Shear, *ACI Structural Journal*, V83, 2, pp. 219-231.